Curvature effect on the radial breathing modes of single-walled carbon nanotubes

Y. Xiao,[1,2] Z. M. Li,[3] X. H. Yan,[1,2,4,*] Y. Zhang,[2] Y. L. Mao,[2] and Y. R. Yang[2]
[1]*College of Science, Nanjing University of Aeronautics and Astronautics, Nanjing 210016, China*
[2]*Department of Physics, Xiangtan University, Xiangtan 411105, Hunan, China*
[3]*Department of Physics, Peking University, Beijing 100871, China*
[4]*Interdisciplinary Center of Theoretical Studies and Institute of Theoretical Physics, CAS, Beijing, 100080, China*
(Received 14 March 2005; revised manuscript received 5 April 2005; published 30 June 2005)

Based on the energy of a relaxed carbon nanotube relative to the graphite sheet (graphene), we construct an analytical correction to the carbon-carbon force constants. Then, the radial breathing modes (RBM) of a number of single-walled carbon nanotubes (SWNTs) are calculated. It is found that for small diameter SWNTs, the curvature effect becomes significant and chirality dependent. Our calculated RBMs are in very good agreement with experimental measurements, especially for ultrasmall diameter SWNTs.

DOI: 10.1103/PhysRevB.71.233405 PACS number(s): 63.22.+m, 61.46.+w

Recently, research on the identifications of the nanotube chirality shows that the radial breathing mode (RBM) is important for the optical and thermal properties of single-walled carbon nanotubes (SWNTs).[1–5] Of them, the fitting formula $\omega_{RBM}=C/d_t$, has been commonly used to describe the diameter dependence of the RBM frequency.[6–15] Although this formula is obtained based on various detailed theoretical calculations, the severe curvature effect invalidates the above simple relationship. This conclusion is experimentally true for 0.4 nm diameter SWNTs produced inside channels of $AlPO_4$-5 (AFI) zeolite crystals.[16] From a fundamental point of view, it is not yet fully clear if the curvature effect would play an important role in RBM. For instance, many different values of the proportionality coefficients C are presented both experimentally and theoretically. Can we propose a universal theoretical explanation to describe the curvature effect on RBM of SWNTs? Consequently, the understanding of the chirality-dependent curvature effect on RBM would be of particular importance for studying the intrinsic properties of each tube chirality. In this paper, we construct the bond-stretching force constant from the scratch, and present an analytical expression of the chirality-dependent curvature effect on RBM. Our calculated results agree well with the experimental measurements of RBMs of 4 Å diameter SWNTs.

The internal strain is built up by rolling up the graphite sheet (graphene) into a tubular structure. The associated strain energy, which is specified as the curvature energy E_c, is defined as the difference of total energy per carbon atom between the tube E_{tube} and the graphene E_g,

$$E_c = E_{tube} - E_g. \tag{1}$$

As is known, the curvature energy E_c has been calculated by using variety of methods, such as density functional theory, classical theory of elasticity, and molecular dynamics.[17–20] All these calculations consistently show that the curvature energy is give by $E_c=D/d_t^2$, where the constant $D\approx 8.4$ eV Å^2. Adams *et al.*[20] have provided an alternative way to describe the curvature energy $E_c=E_0(1-\cos\phi)$ with $E_0=4.17$ eV. The planarity ϕ is a structural parameter, which is the angle between the π orbitals of neighboring atoms. For the graphene, we have $E_g=-10.6$ eV with respect to a nonspin-polarized carbon atoms using density functional calculations implemented with CASTEP.[21] Now, we define E_{tube} to be

$$E_{tube} = \left[1 + \frac{E_0}{E_g}(1-\cos\phi)\right]E_g = AE_g, \tag{2}$$

where $A=6.43/10.6+(4.17/10.6)\cos\phi$. Then, the bond-stretching force constant K_{tube} that corresponds to the equilibrium configuration of SWNTs is in the form of

$$K_{tube} = \left.\frac{\partial^2 E_{tube}}{\partial r^2}\right|_{r_g+u} = A\left.\frac{\partial^2 E_g}{\partial r^2}\right|_{r_g+u} = A\left(\left.\frac{\partial^2 E_g}{\partial r^2}\right|_{r_g} + u\left.\frac{\partial^3 E_g}{\partial r^3}\right|_{r_g}\right), \tag{3}$$

where r_g and $r_{tube}=r_g+u$ are the equilibrium distances of the carbon-carbon bonds in graphene and SWNTs, respectively. Note that the first term in the bracket is simply the bond-stretching force constant of graphene K_g, we have

$$K_{tube} = AK_g + A(r_{tube}-r_g)\left.\frac{\partial^3 E_g}{\partial r^3}\right|_{r_g}. \tag{4}$$

Since the explicit functional dependence of the energy E_g on the atomic displacements is unknown, we make a particular choice: the Morse potential, so that

$$E_g = U[e^{-2(r-r_0)/b} - 2e^{-(r-r_0)/b}], \tag{5}$$

where U is the cohesion energy per bond, and r_0 is the equilibrium bond length. To make it comparable to that of graphite and diamond,[22] we take $U=3.7$ eV. The constant b is chosen to obtain the correct bond-stretching force constant. In a force constant model, the first and second nearest neighboring bond-stretching force constants are $K_g^1=22.78$ eV Å^2 and $K_g^2=5.49$ eV Å^2, respectively.[2] The corresponding values of b are 0.57 and 1.16, as deduced from the Morse potential. Substituting the Morse potential to the second term of Eq. (4), we obtain

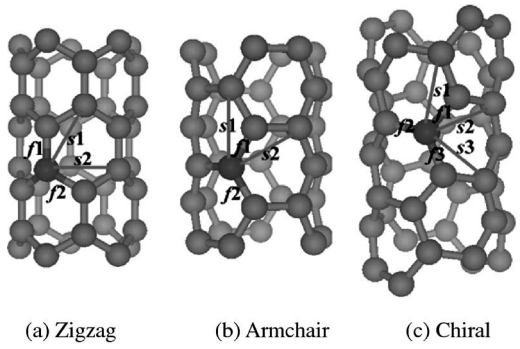

FIG. 1. The first and second nearest neighboring bonds (a) for zigzag, (b) for armchair, and (c) for chiral SWNTs.

$$K_{tube} = AK_g + 6AU(r_g - r_{tube})/b^3. \quad (6)$$

One finds that the radial force constant is determined by two competing contributions: a softened force constant of graphene and the structural difference between SWNTs and graphene. It is seen that K_g is softened by the factor A when rolling up the graphene into a nanotube. From the second term, one can see that the force constant, hereby the RBM frequency, is directly related to the elongation or shortening of carbon-carbon bonds along the circumferential direction. The change of bond length, induced by rolling up the graphene plane, is thus dependent on the chirality. So Eq. (6) predicts that ω_{RBM} is not only diameter dependent, but also chirality dependent. In addition, the electronic effects on the force constant K_{tube} are included in the factor A, which reflects the interaction of π orbitals between neighboring atoms. Such an interaction induces obvious softening in the total energy and force constant as seen in Eq. (6). Moreover, the σ^*-π^* hybridizations have been introduced in very small diameter tubes.[16] However, the *ab initio* calculations[18,19] reproduce the relation $E_c = D/d_t^2$ with $D \approx 8.4$ eV Å^2 and thus Eq. (6) is still valid for these small diameter tubes.

In order to take the curvature effect into account, we calculate the RBM within a force constant model[2,23,24] using Eq. (6). We consider the first and second nearest neighboring carbon atoms for the graphene and SWNTs in our calculations. For graphene, we have $r_g^1 = 1.42$ Å and $r_g^2 = 2.46$ Å, while r_{tube}^1 and r_{tube}^2 can be obtained from the geometrical structure optimizations in first-principles calculations.[25–27] As shown in Fig. 1, there are three and six carbon bonds corresponding to the first and second nearest neighboring carbon atoms. For a general $(n,0)$-zigzag or (n,n)-armchair SWNTs, its symmetry group contains the horizontal and vertical mirror reflections. This means that two nearest bonds $(f1,f2)$ and two second nearest bonds $(s1,s2)$ are representative. Considered its symmetry group includes a twofold horizontal rotation for a general chiral tube, it is necessary to choose all three nearest bonds $(f1,f2,f3)$ and three second nearest bonds $(s1,s2,s3)$ in our calculations.

In Fig. 2, we apply the above scheme to calculate the softening coefficient A as a function of tube diameter. The value of A increases with the increasing diameter and approaches 1.0 for the SWNTs with diameter larger than 3 nm. So, K_{tube} would be governed by the K_g from Eq. (6) for large diameter tubes and RBM can be calculated by borrowing the force constants from graphene, as reported previously.[2,23,24] However, the effect of coefficient A and the distortion of carbon bonds become significant for the small diameter tubes. Taking (5, 0) and (4, 2) SWNTs for example, their calculated RBMs by adopting ideal graphene force constants are systematically higher than the experimental values by ~ 20 cm^{-1}.[28] By looking at the fully relaxed nanotube coordinates, one can find that the length of carbon-carbon bonds "along" the tube axis [$f1$ for (5, 0) tube and $f3$ for (4, 2) tube] is shorter than those bonds that are "around" the tube circumference (see Table I). Such a phenomenon can be attributed to the pronounced curvature effect for these ultrasmall diameter SWNTs. In particular, the bond alternation is more significant for the (5, 0) tube, since (5, 0) tube has the smallest chiral angle between these two SWNTs.

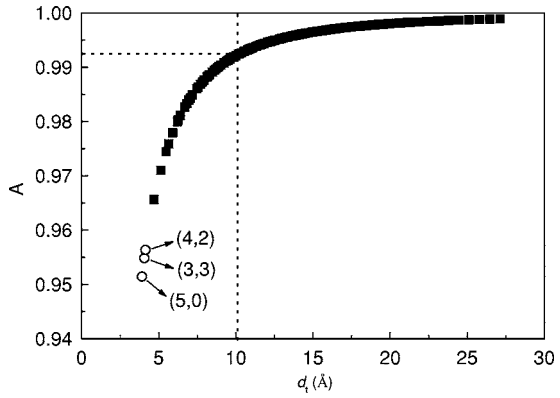

FIG. 2. The value of A as a function of tube diameter. The open circles represent the value of A for (5, 0), (4, 2), and (3, 3) tubes.

By virtue of bond lengths and Eq. (6), we calculated the RBM frequencies of (5, 0), (4, 2), and (3, 3) SWNTs, and compared our results with experimentally observed modes and other theoretical calculations in Table II. The 4 Å diameter SWNTs in AFI were confirmed by high-resolution transmission electron microscopy and there were only nanotubes with three different chirality: (5, 0), (4, 2), and (3, 3). Furthermore, the tube chirality of samples can be distinguished by very different absorption and photoluminescence spectra.[16] The (3, 3) tube has its lowest absorption band around 3.0 eV, which is far away from the resonance region

TABLE I. The bond length (in angstroms) of RBM of (5, 0) and (4, 2) SWNTs from density functional calculations. See text for meanings of the bond parameters.

	(5, 0)		(4, 2)	
$f1$	1.40[a]	1.41[b]	1.44[a]	1.44[b]
$f2$	1.45[a]	1.45[b]	1.44[a]	1.44[b]
$f3$			1.42[a]	1.42[b]
$s1$	2.47[a]	2.48[b]	2.46[a]	2.46[b]
$s2$	2.40[a]	2.40[b]	2.42[a]	2.42[b]
$s3$			2.46[a]	2.46[b]

[a]Reference 26.
[b]Reference 27.

TABLE II. The RBM frequency (in cm^{-1}) used to fit the observed Raman modes of 4 Å diameter SWNTs in zeolite crystals in comparison to our calculated results (underlined values).

Observed modes	510[a]		550[a]	
	514[b]		545[b]	
	515[c]		548[c]	
Calculated for (5, 0)	**547**	525[d]	562[a]	536[c]
Calculated for (4, 2)	**513**	529[d]	530[a]	538[c]
Calculated for (3, 3)	**528**	538[d]	541[a]	

[a]Reference 28.
[b]Reference 29.
[c]Reference 30.
[d]Reference 26.

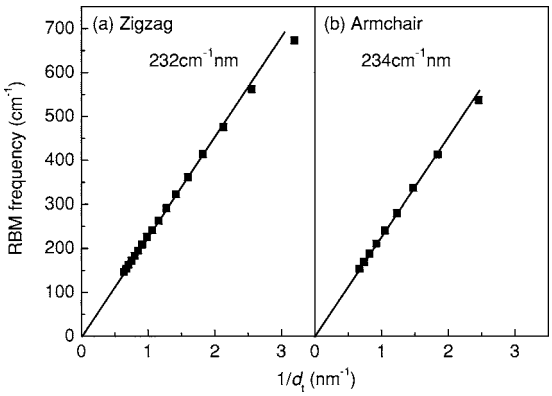

FIG. 3. Frequencies of the RBM of a number of SWNTs for (a) zigzag and (b) armchair tubes. The solid lines are a linear fit to the data for the large diameter SWNTs.

for the excitation laser energy, thus its RBM is negligibly weak.[28,29] So, only (5, 0) and (4, 2) tubes are related to these two strong peaks in the Raman spectra, which are around at 510 and 550 cm^{-1} as seen in Table II.[28–30] Comparing the observed modes with our calculated RBM for (5, 0) and (4, 2) tubes, we can clearly assign the peak at 510 cm^{-1} with (4, 2) tube, while the peak at 550 cm^{-1} with (5, 0) tube. From Table II, it is seen that our calculated RBM frequencies are in better agreement with the observed modes than other calculations. The good agreement indicates that curvature effect on RBM has been properly incorporated in Eq. (6). In addition, the underestimated frequency (about 20 cm^{-1}) can be attributed to the AK_g term and structural term from Eq. (6). The AK_g and structural contributions to the RBM are −10 and −7 cm^{-1} for the (4, 2) tube, while −13 and −2 cm^{-1} for the (5, 0) tube. The difference of the structural contribution between (5, 0) and (4, 2) tubes arises from the curvature effect on the bonds along the circumferential direction.

To give further insight into the curvature effect, we show the RBM frequencies of even smaller diameter SWNTs in Table III. The RBM frequencies calculated with Eq. (6) are systematically lower than that without Eq. (6) except the (2, 2) tube. From the geometry optimization with CASTEP,[31] one can see that the relaxed structure of the (2, 2) tube shows significant deviations from the ideal rolled graphene sheet configuration. The large structural difference results in the dominating contribution of the second term in Eq. (6) and thus a higher frequency than the ideal value. In addition, it is noted that the calculated RBM frequency of (3, 1) tube is 755 cm^{-1}, which is very consistent with the position of a Raman peak (760 cm^{-1}) observed recently for SWNTs in even smaller zeolite crystals (≈6 Å) than AFI (≈7 Å).[32] Due to even smaller diameter of this zeolite crystal, the existence of SWNTs with less than 4 Å diameter is predicted and this peak at 760 cm^{-1} may be attributed to the SWNTs in these zeolite crystals. The details of the fabrication process and Raman spectra measurement of SWNTs in this zeolite crystal would be presented elsewhere. Based on our calculations, we conclude that the peak may be associated with the (3, 1) tube.

TABLE III. The RBM frequency (in cm^{-1}) for 3–4 Å diameter SWNTs calculated with Eq. (6) and without Eq. (6).

(n,m)	(4, 2)	(3, 3)	(5, 0)	(4, 1)	(3, 2)	(4, 0)	(3, 1)	(2, 2)
ω_{cal}[a]	513	528	547	589	635	671	755	828
ω_{cal}[b]	530	541	562	611	640	695	764	790

[a]Calculation with Eq. (6).
[b]Calculation without Eq. (6).

We calculate in Fig. 3 the RBM frequencies of a number of zigzag ($n=4-20$) and armchair ($n=3-11$) SWNTs based on optimized tube structures.[25] Not surprisingly, the calculated RBM frequencies are almost inversely proportional to the diameter for large diameter SWNTs.[33–35] A fit to $\omega_{RBM}=C/d_t$ yields $C=232/d_t$ cm^{-1} nm for zigzag and $C=234/d_t cm^{-1}$ nm for armchair SWNTs, which are larger than that calculated from K_g.[2,23,24] The values of C for armchair and zigzag SWNTs are in agreement with that from density functional calculations.[11] The difference of C between two types of tubes is due to the fact that the magnitudes of increase or decrease in bond lengths are very different. More importantly, such a difference reveals that RBM is also dependent on chirality, especially for SWNTs of diameter less than 1 nm.

In summary, we investigate the curvature effect on RBM of SWNTs by constructing an analytical correction to the carbon-carbon radial force constants. By introducing the curvature energy, we present the nanotubes' force constants, which are related to the graphene's force constants and structural changes. Our calculated results show that the curvature effect is small for large diameter SWNTs, while it becomes significant for small diameter SWNTs, especially for ultrasmall diameter tubes. We predict that the RBM frequency is both diameter and chirality dependent due to the curvature effects. Moreover, our calculated RBMs are in very good agreement with experimental measurements, compared with other calculations.

We would like to thank Professor Ado Jorio for making their results available prior to publication. We also thank

Dr. Viktor Zolyomi for sending us their structural data of nanotubes. This work was supported by the Program for New Century Excellent Talents in University (Grant No. NCET-04-0779) and Science & Technology Foundation for Ministry of Education (No. 204099), and by the Scientific Research Fund of Hunan Provincial Education Department (Nos. 03A046, 03JZY3019, and 04C647), and partly by the Undergraduate Innovation Fund of Xiangtan University.

*Author to whom correspondence should be addressed; electronic address: xhyan@nuaa.edu.cn

[1] S. Reich, C. Thomsen, and J. Maultzsch, *Carbon Nanotubes: Basic Concepts and Physical Properties* (Wiley-VCH, Cambridge, 2004).
[2] R. Saito, G. Dresselhaus, and M. S. Dresselhaus, *Physical Properties of Carbon Nanotubes* (Imperial College Press, London, 1998).
[3] G. D. Mahan and G. S. Jeon, Phys. Rev. B **70**, 075405 (2004).
[4] Yu. N. Gartstein, Phys. Lett. A **327**, 83 (2004).
[5] G. D. Mahan, Phys. Rev. B **65**, 235402 (2002).
[6] S. M. Bachilo, M. S. Strano, C. Kittrell, R. H. Hauge, R. E. Smalley, and R. B. Weisman, Science **298**, 2361 (2002).
[7] A. Jorio, R. Saito, J. H. Hafner, C. M. Lieber, M. Hunter, T. McClure, G. Dresselhaus, and M. S. Dresselhaus, Phys. Rev. Lett. **86**, 1118 (2001).
[8] R. Pfeiffer, H. Kuzmany, Ch. Kramberger, Ch. Schaman, T. Pichler, H. Kataura, Y. Achiba, J. Kurti, and V. Zolyomi, Phys. Rev. Lett. **90**, 225501 (2003).
[9] Ch. Kramberger, R. Pfeiffer, H. Kuzmany, V. Zolyomi, and J. Kurti, Phys. Rev. B **68**, 235404 (2003).
[10] S. Bandow, S. Asaka, Y. Saito, A. M. Rao, L. Grigorian, E. Richter, and P. C. Eklund, Phys. Rev. Lett. **80**, 3779 (1998).
[11] J. Kurti, G. Kresse, and H. Kuzmany, Phys. Rev. B **58**, R8869 (1998).
[12] H. Telg, J. Maultzsch, S. Reich, F. Hennrich, and C. Thomsen, Phys. Rev. Lett. **93**, 177401 (2004).
[13] Ge. G. Samsonidze, R. Saito, N. Kobayashi, A. Gruneis, J. Jiang, A. Jorio, S. G. Chou, G. Dresselhaus, and M. S. Dresselhaus, Appl. Phys. Lett. **85**, 5703 (2004).
[14] A. Jorio, C. Fantini, M. A. Pimenta, R. B. Capaz, G. G. Samsonidze, G. Dresselhaus, M. S. Dresselhaus, J. Jiang, N. Kobayashi, A. Gruneis, and R. Saito, Phys. Rev. B **71**, 075401 (2005).
[15] M. Damnjanovic, E. Dobardzic, and I. Milosevic, J. Phys.: Condens. Matter **16**, L505 (2004).
[16] Z. M. Li, Z. K. Tang, H. J. Liu, N. Wang, C. T. Chan, R. Saito, S. Okada, G. D. Li, J. S. Chen, N. Nagasawa, and S. Tsuda, Phys. Rev. Lett. **87**, 127401 (2001).
[17] D. Sanchez-Portal, E. Artacho, J. M. Soler, Angel Rubio, and P. Ordejon, Phys. Rev. B **59**, 12678 (1999).
[18] O. Gulseren, T. Yildirim, and S. Ciraci, Phys. Rev. B **65**, 153405 (2002).
[19] I. Cabria, J. W. Mintmire, and C. T. White, Phys. Rev. B **67**, 121406(R) (2003).
[20] G. B. Adams, O. F. Sankey, J. B. Page, M. O. Keeffe, and D. A. Drabold, Science **256**, 1792 (1992).
[21] Y. L. Mao, X. H. Yan, Y. Xiao, J. Xiang, Y. R. Yang, and H. L. Yu, Phys. Rev. B **71**, 033404 (2005).
[22] W. A. Harrison, *Electronic Structure and the Properties of Solids* (Freeman, San Francisco, 1980).
[23] Z. M. Li, V. N. Popov, and Z. K. Tang, Solid State Commun. **130**, 657 (2004).
[24] J. X. Cao, X. H. Yan, Y. Xiao, Y. Tang, and J. W. Ding, Phys. Rev. B **67**, 045413 (2003).
[25] J. Kurti, V. Zolyomi, M. Kertesz, and G. Y. Sun, New J. Phys. **5**, 125 (2003).
[26] H. J. Liu and C. T. Chan, Phys. Rev. B **66**, 115416 (2002).
[27] M. Machon, S. Reich, C. Thomsen, D. Sanchez-Portal, and P. Ordejon, Phys. Rev. B **66**, 155410 (2002).
[28] Z. M. Li, Z. K. Tang, G. G. Siu, and I. Bozovic, Appl. Phys. Lett. **84**, 4101 (2004).
[29] M. Hulman, H. Kuzmany, O. Dubay, and G. Kresse, J. Chem. Phys. **119**, 3384 (2003).
[30] I. L. Li, G. D. Li, H. J. Liu, C. T. Chan, and Z. K. Tang, Appl. Phys. Lett. **82**, 1467 (2003).
[31] Y. L. Mao, X. H. Yan, Y. Xiao, J. Xiang, Y. R. Yang, and H. L. Yu, Nanotechnology **15**, 1000 (2004).
[32] J. P. Zhai (unpublished).
[33] C. Fantini, A. Jorio, M. Souza, M. S. Strano, M. S. Dresselhaus, and M. A. Pimenta, Phys. Rev. Lett. **93**, 147406 (2004).
[34] H. Son, Y. Hori, S. G. Chou, D. Nezich, Ge. G. Samsonidze, G. Dresselhaus, M. S. Dresselhaus, and E. B. Barros, Appl. Phys. Lett. **85**, 4744 (2004).
[35] A. G. Souza Filho, S. G. Chou, G. G. Samsonidze, G. Dresselhaus, M. S. Dresselhaus, L. An, J. Liu, A. K. Swan, M. S. Unlu, B. B. Goldberg, A. Jorio, A. Gruneis, and R. Saito, Phys. Rev. B **69**, 115428 (2004).